Genetic Algorithms and Method of Moments (GA/MOM) for the Design of Integrated Antennas

J. Michael Johnson, *Member, IEEE*, and Yahya Rahmat-Samii, *Fellow, IEEE*

***Abstract*— This paper introduces a novel technique for efficiently combining genetic algorithms (GA's) with method of moments (MoM) for integrated antenna design and explores a two example applications of the GA/MoM approach. Integral to efficient GA/MoM integration is the use of direct Z-matrix manipulation (DMM). In DMM a "mother" structure is selected and its corresponding impedance or Z-matrix is filled only once prior to beginning the GA optimization process. The GA optimizer then optimizes the design by creating substructures of the *mother* structure as represented by the corresponding subsets of the original *mother* Z-matrix. Application of DMM with GA/MoM significantly reduces the total optimization time by eliminating multiple Z-matrix fill operations. DMM also facilitates the use of matrix partitioning and presolving to further reduce the optimization time in many practical cases. The design of a broad-band patch antenna with greater than 20% bandwidth and a dual-band patch antenna are presented as examples of the utility of GA/MoM with DMM. Measured results for the dual-band antenna are compared to numerical results. Excellent agreement between numerical and measured results is observed.**

***Index Terms*—Genetic algorithms, method of moments, multiband patch antennas.**

I. Introduction

As wireless systems continue to enjoy increased application and gain wider acceptance, performance and cost constraints on the antennas employed by these systems become more difficult to meet. Antennas that are conformal or low profile and that exhibit broad-band or multiband operation are of particular interest for many of these new systems. Concomitant with increased performance levels is the need for antenna designs with the potential for low cost manufacturing. To address the requirements and the severe constraints imposed by commercial application of these antennas, new innovative antenna design methodologies are required.

To date, most new wireless system antenna designs have been derived from existing canonical designs such as the monopole or the $\frac{1}{2}$ and $\frac{1}{4}$ wavelength patch antennas. Generally speaking, these new designs, especially those exhibiting wide-band or multiband operation, have been developed through the careful application of engineering judgment and expertise to extend the canonical designs and/or through serendipitous discovery [1]. Either way, the development of new designs is often a slow haphazard process that often yields designs that are difficult to manufacture and, therefore, unsuitable for commercial wireless antenna applications.

What is needed is a new approach that allows the designer to specify design goals and then generate a candidate "optimal" structure in a methodical and evolutionary manner. An approach that holds much promise in this regard is the coupling of full wave electromagnetic modeling codes with optimization methods.

Recently, several investigators have reported encouraging results from the coupling of a relatively new optimization technique known as the genetic algorithm (GA) with method of moments (MoM). In particular, [2] reported the design of compact microwave filters using GA coupled with a 2.5 D MoM analysis technique and [3] and [4] reported some interesting results of applying the well known numerical electromagnetic code (NEC) and GA to the design of circularly polarized wire antennas with broad angular coverage. In both of these cases, the results obtained from the GA optimization exhibited excellent performance for the selected optimization parameters. In addition to producing results with excellent performance, these examples also produced in entirely unconventional and nonintuitive physical realizations.

In this paper, a novel integration of GA and MoM for the design of low-cost integrated antennas is described. Essentially, GA/MoM amounts to a tailored MoM combined with a GA search within the solution domain afforded by the MoM results. Section II discusses the specifics of the GA optimizer and the implementation of MoM used herein and Section III describes the direct Z-matrix manipulation (DMM) integration of GA and MoM (GA/MoM) including the approach to matrix partitioning and presolving facilitated by DMM. As a demonstration of the applicability of GA/MoM for patch antenna design, two patch antenna designs are presented. A broad-band patch antenna design is described in Section IV and a dual-band patch antenna design is described in Section V. Measured data for a prototype dual-band antenna that compares favorably with the numerical results is also provided in Section V. Finally, the operation of the dual-band design is investigated in some detail to give some additional insight into the typically unintuitive designs that are often produced by the GA/MoM approach.

II. GA and the Method of Moments

The GA/MoM integration method discussed utilizes direct manipulation of the Z-matrix (DMM) to significantly reduce

Manuscript received September 30, 1997. This work was supported in part by DARPA under Contract JFBI94-222/J4C942220, in part by Rockwell/MICRO, and in part by MURI contract DAAH04-96-1-0389.

J. M. Johnson is with the Department of Electrical Engineering, University of Nevada, Reno, NV 89557-0153 USA.

Y. Rahmat-Samii is with the Department of Electrical Engineering, University of California at Los Angeles, CA 90095-1594 USA.

Publisher Item Identifier S 0018-926X(99)09392-8.

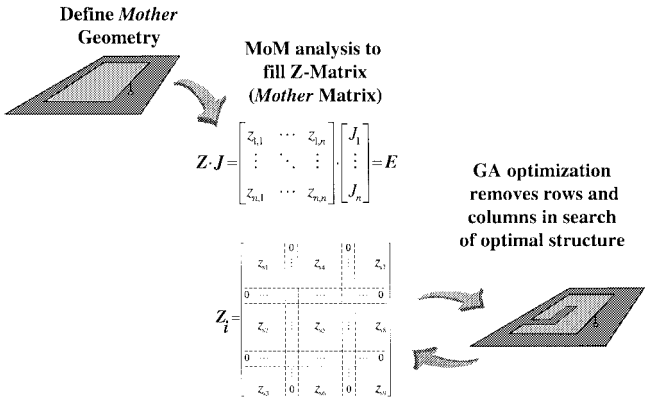

Fig. 1. After selection of a *mother* structure and the filling of a *mother* Z-matrix, the optimization consists of using GA to search among the set of substructures that can be constructed by removing rows and columns from the *mother* Z-matrix, which corresponds to removing metal from the mother structure.

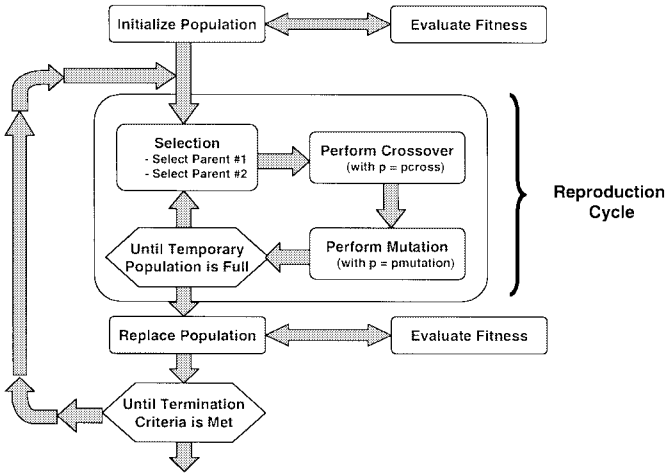

Fig. 2. Block diagram of a simple generational GA optimizer.

the computational cost in the optimization process compared to previously reported GA/MoM approaches. In the DMM approach, a *mother* structure is selected. The GA optimization then searches for an optimal substructure contained within the *mother* structure that comes closest to meeting the design goals. This concept is illustrated in Fig. 1. The reduction of the GA optimization task to one involving substructures of a *mother* structure provides a significant timesaving in that the Z-matrix used in the MoM calculations is only filled once at the beginning of the optimization instead of at each optimization iteration. DMM also facilitates the use of matrix partitioning and presolving to further reduce the solve time for some problems.

As discussed above and indicated in Fig. 1, the GA/MoM approach presented in this paper combines a tailored MoM analysis with an iterative GA-based search for an optimal solution. A tutorial introduction to GA optimization and its application to various electromagnetic problem is presented in [5]. GA's have been applied to a wide range of electromagnetic problems including the design of broad-band multilayer absorbers, array design, and remote sensing [6]–[12].

In the case of GA/MoM, the population consists of a set of substructures and the chromosomes of the individuals in the population describe the physical characteristics of the individuals. The fitness function involves the application of MoM to the individual substructures followed by a weighted summation of the information produced by the MoM analysis.

A block diagram of the generational GA optimizer used is illustrated in Fig. 2. The selection strategy used here in GA/MoM is known as binary tournament selection [13]. In tournament selection, a subpopulation of N individuals $(N = 2)$ is chosen at random from the population. The individuals of this subpopulation then *compete* on the basis of their fitness. The individual in the subpopulation with the highest fitness *wins the tournament* and becomes the selected individual. Further details of the implementation of a GA optimizer and the various operators involved are covered in detail in [6], [14].

The other part of the GA/MoM approach is a tailored MoM analysis. Since the majority of antenna structures can be reasonably well described by a set of wires, sources, and metal plates, an electric field integral equation (EFIE)-based MoM provides considerable flexibility.

EFIE/MoM [6], [15] is a well-established full wave method for evaluating the performance of arbitrarily shaped electromagnetic structures consisting of wires and electrically thin metal plates. The method involves subdividing the metal surfaces and wires in the modeled structures. The general problem is reduced to that of solving a set of linear equations of the form,

$$ZI = V \tag{1}$$

where Z is the Z-matrix or impedance matrix that specifies the relationship between the various surface patches and wire segments in the problem, V is a vector accounting for sources, and I is a vector containing the unknown currents that are to be found.

An excellent choice of testing and basis functions for GA/MoM is the Rao–Wilton–Glisson (RWG) basis function set developed in [16]. The RWG basis function set has the advantage of not requiring different basis functions for boundary elements and interior elements and is designed to be used with triangular surface patches. The wire elements can be modeled adequately by triangular basis functions [17]. An important modification, especially important in small structures, involves the balancing of currents at any wire/surface junctions to ensure continuity of current as required by Kirchoff's current law. In addition, a straightforward modification of the Green's function in the EFIE enables the inclusion of infinite ground planes.

III. GA/MOM Integration

GA/MoM begins with the selection of a *mother* structure and then derives substructures from the *mother* structure through an iterative GA search with MoM as the basic analytical method for evaluating the performance of these substructures. Having summarized the basic elements GA and MoM, the GA/MoM integration is presented in this section.

For GA/MoM, let the substructures allowed in the search space be those that can be produced by removing metal of the

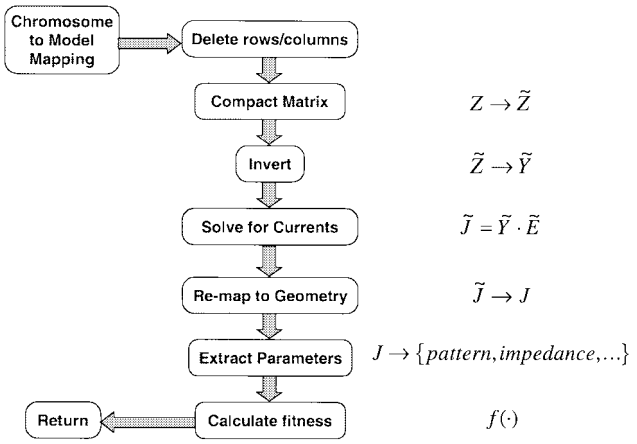

Fig. 3. GA/MoM combines a GA optimization with a tailored MoM analysis, which involves removal of rows and columns from the Z-matrix instead of refilling the Z-matrix at each GA iteration.

original structure. Removal a portion of the metal is equivalent to forcing the currents on that portion of the *mother* structure to be identically zero. This, in turn, is equivalent to setting the corresponding basis elements in the *mother* structure Z-matrix to zero leaving rows and columns in the Z-matrix filled with zeros. In practice, these zero rows and columns in the Z-matrix make the matrix singular. Since the direct analysis of a given substructure by MoM would simply not include regions without metal, it is quickly realized that the substructure Z-matrix can be produced from the *mother* Z-matrix by removing the rows and columns associated with the removed metal. The removal of these rows and columns leaves a nonsingular matrix that can be used to find the unknown currents on the substructure.

An optimization methodology as depicted in Fig. 3, can, therefore, be considered. In this methodology, a *mother* Z-matrix is constructed that includes the presence of metal everywhere that metal might allowed to be. All possible structures that can be constructed from this *mother* configuration then become substructures of this *mother* configuration. The Z-matrices of these subset configurations likewise are realized to be submatrices of the *mother* Z-matrix. Put simply, the Z-matrix of any substructure can be derived from that of the *mother* structure by simply removing the rows and columns of the matrix corresponding to the pieces of metal that are being removed. The remaining matrix elements are unchanged by this removal of elements.

An exception to this rule is that the matrix elements that are formed by junctions between wire segments and metal patches. In these instances, the entries in the Z-matrix are dependent on other rows and columns due to the necessary application of Kirchoff's current law to relate the surface currents in the surface patches and the wires attached thereto. This exception is easily overcome by excluding these "dependent" rows and columns from the group of "removable" rows and columns. Excluding certain rows and columns from the "removable" group in turn excludes a subset of substructures from being considered during the GA search. In practice, this is a minor limitation.

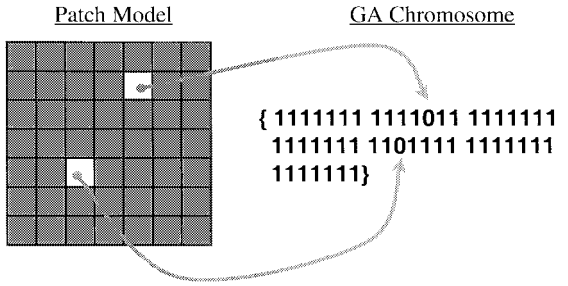

Fig. 4. The relationship between the physical problem and the chromosome is simply a mapping between patches of metal and a binary string such that a "1" indicates the presence of metal and a "0" indicates the absence of metal.

Therefore, for all intents and purposes the Z-matrix for all substructures of the original *mother* structure can be formed by simply removing rows and columns from the *mother* Z-matrix, voltage vector and current vectors of (1). A solution methodology is then apparent that allows for the exploration of a large number of potential configurations without the need for costly re-execution of the Z-matrix filling operations.

From the GA viewpoint, the chromosome can be a simple binary string of ones and zeros, one bit for each "removable" subsection in the *mother* structure. A "0" in the chromosome then represents the absence of metal while a "1" represents the presence of metal. This is illustrated in Fig. 4. The fitness function then involves solving a $ZI = V$ equation for a submatrix derived from the original, *mother* Z-matrix and then extracting the appropriate parameters from the results to compare with the optimization goals.

Referring to Fig. 3, a submatrix, $\tilde{Z}$, is created from the *mother* Z-matrix by removing the rows and columns corresponding to a mapping of the zeros in the chromosome to metal regions in the model. The $\tilde{Z}\tilde{I} = \tilde{V}$ equation is then solved and the resulting current vector is used to extract the desired parameters such as input impedance or antenna pattern. Since the method involves direct operation on the mother Z-matrix the method has been named the DMM method.

GA/MoM then reduces to a two-step process. The first step is the standard matrix filling operation of MoM in which *mother* Z-matrices are constructed and stored for each frequency of interest. The second step is the GA optimization utilizing the previously filled MoM matrices or submatrices.

The DMM method avoids the cost of refilling the Z-matrix at each re-evaluation of the fitness function, a cost that can be substantial. Fig. 5 shows the typical times involved in filling and subsequently solving a typical MoM problem relative to the number of unknowns involved. For the typical problem with less than about 200 unknowns, fill time is on the order of the solve time in this case. This timesaving can be particularly important when considering an optimization problem that may involve a large number of successive MoM evaluations. Considering a problem involving 100 unknowns, and where a population of 100 individuals and 100 generations, the total time saved by not refilling the matrix as outlined above amounts to 133 min on a 200-MHz Pentium Pro. In other words, with the DMM methodology proposed above, a total optimization time of approximately 50 min results as opposed to 183 min without the application of DMM.

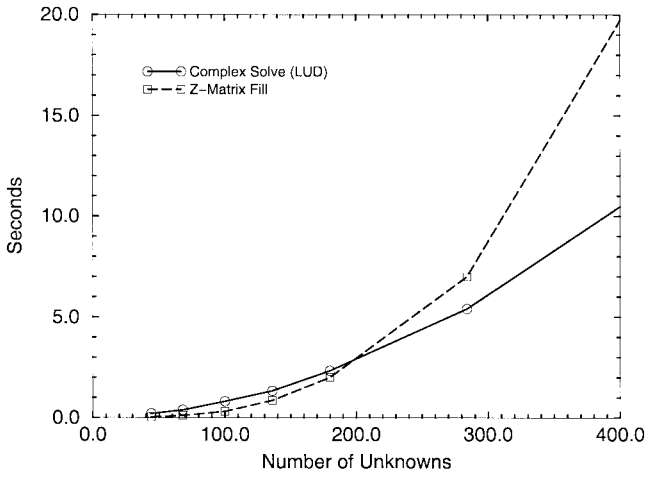

Fig. 5. Matrix fill time and matrix inversion time comparison (on a 200-MHz Pentium Pro).

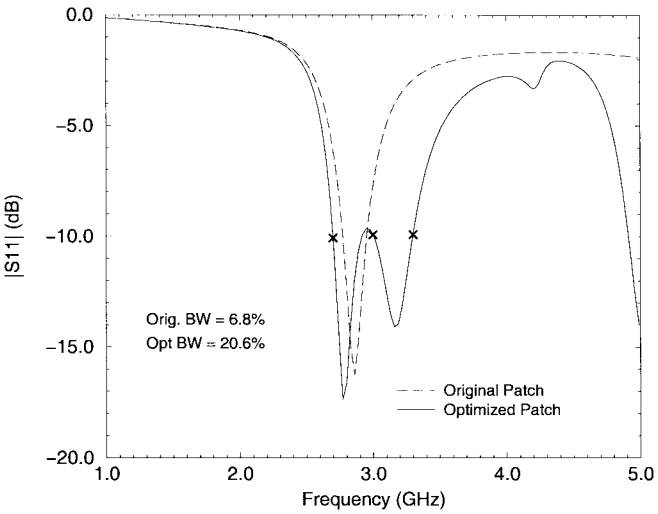

Fig. 6. Calculated $S11$ for patch antenna before and after GA/MoM optimization.

Having adopted the DMM approach a second computational cost saving methodology can be exploited by using matrix partitioning. Many practical problems involve portions of a given modeled structure that are modified during optimization along with portions that are not modified. This characteristic can be exploited to achieve further execution timesaving by partitioning the matrix equation and "presolving" a portion of the equation associated with the elements that are not changed [18]. If the problem is partitioned such that the elements that do not change or are always present and are always located in the lower right corner of the matrix, the equation can be solved as outlined in (2)–(6). With partitioning, (1) becomes

$$\begin{bmatrix} Z_{mm} & Z_{cm} \\ Z_{mc} & Z_{cc} \end{bmatrix} \begin{bmatrix} I_m \\ I_c \end{bmatrix} = \begin{bmatrix} V_m \\ V_c \end{bmatrix} \tag{2}$$

where the subscript m refers to elements that may be modified (removed) during optimization and c refers to elements that are constant during optimization. After partitioning, the matrix equation (2) can be solved for I_c, as given in (3) and (4)

$$Y_{cc} = Z_{cc}^{-1} \tag{3}$$

$$I_c = Y_{cc} \cdot \{V_c - Z_{mc} I_m\}. \tag{4}$$

Then substituting this result back into (2) and solving for I_c the results, after some simple algebra, are given by (5) and (6)

$$Y_{mm} = \{Z_{mm} - Z_{cm} Y_{cc} Z_{mc}\}^{-1} \tag{5}$$

$$I_m = Y_{mm} \{V_m - Z_{cm} Y_{cc} V_c\}. \tag{6}$$

Counting the number of complex multiplication operations necessary to repeatedly solve the system represented by the original matrix equation (2) relative to the result of presolving for Y_{cc} using (3) followed by (4)–(6) it is clear that when *the number of elements that are modified* is less than or equal to *number of elements that are held constant*, the application of matrix partitioning and presolving can yield significant savings in computation time.

The GA/MoM method described above has been applied to several antenna optimization problems involving patches and wires.

IV. Example 1: Wide-Band Patch Antenna Design

As a first example of the application of GA/MoM for antenna design, consider the design of a broad-band patch antenna. Usually broad-band patch designs are achieved by adding passive resonating elements to a basic design leading to antennas that are usually much larger and/or more complicated to build and tune. The goal here was to produce a patch antenna that has an acceptable, 2 : 1 VSWR, match over a 20% bandwidth centered at 3 GHz. As can be seen in Fig. 6, the initial match, as indicated by a dotted line, has a bandwidth of approximately 6%. The original patch design consisted of a 5.0 × 5.0 cm patch suspended 0.5 cm above an infinite ground plane. The feed was modeled as a wire with a voltage source at the ground plane/wire interface and located 2.5 × 1.25 cm from the corner of the patch. The original patch structure including the triangularization used is shown in Fig. 7(a).

A *mother* matrix for the original design was formed and GA optimization was performed by iteratively removing square metal subsections from the patch region and the corresponding rows and columns from the Z-matrix as outlined above in Section IV. The population size was 100 individuals and 100 generations were evaluated. Probability of crossover was 0.7 while the probability of mutation was equal to 0.02. Elitism and binary tournament selection were used. The goal was to minimize the maximum $S11$ magnitude at three frequencies, 2.7 GHz, 3 GHz, and 3.3 GHz. The fitness function in this case was given by

$$\textit{fitness} = \min_{\forall n}(S11_n) \tag{7}$$

where the subscript n refers to sample points in the $S11$ versus frequency function. The MoM step was used to generate a set of three Z-matrices for the *mother* configuration, one for each frequency. The GA optimizer then iteratively removed rows and columns from these three *mother* matrices in search of a solution. Metal removal was constrained to be square patches through the mapping from the GA chromosome to the Z-matrix entries.

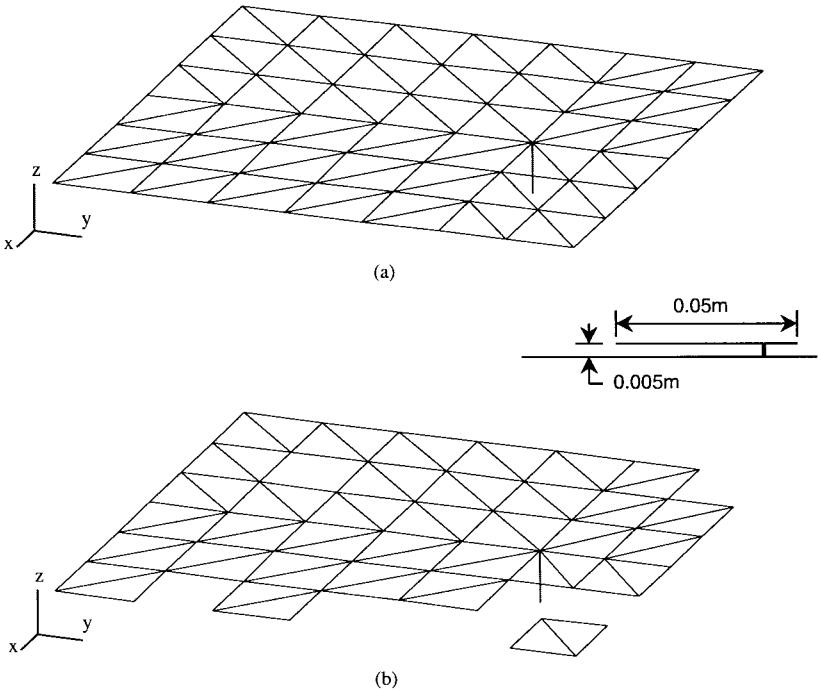

Fig. 7. Patch antenna with simple wire feed above an infinite ground plane (not shown). (a) Original square patch. (b) Patch configuration resulting from GA optimization.

The results of the best individual encountered during the GA/MoM optimization in terms of magnitude $S11$ are shown in Fig. 6 as a solid line. As can be seen, an acceptable $2:1$ match has been achieved over the entire 2.7–3.3-GHz band. The resulting optimized structure is shown Fig. 7(b). While not an intuitive result, the design is readily realizable by standard printed circuit board techniques.

Of course, the antenna pattern produced by the resulting unsymmetrical structure may not be suitable for some applications. In particular, the lack of symmetry in the patch design results in a slightly asymmetric pattern and a high cross-polarization component.

As an aside, approaching these designs through an exhaustive manual trial and error method might be considered. In the first case, there are 72 triangular patches grouped into 36 square subpatches. This means that there are 2^{36} or 68.7×10^9 possible combinations of this design. The GA approach required less than 3×10^3 solutions of the $ZI = V$ equation to find a good result.

V. Example 2: Dual-Band Patch Antenna Design

As a second example of the application of the GA/MoM design methodology consider the design of a dual-band patch antenna. Such a dual-band antenna would be useful in wireless applications that combine cellular and satellite operation in a single unit. In the case presented here, the design goal was to produce an antenna that has a good match at two frequencies—3.0 and 4.0 GHz. Starting with the same patch antenna as in the previous example the GA/MoM optimization was applied with the goal of minimizing the return loss at the two design frequencies. The fitness function of (9) was used.

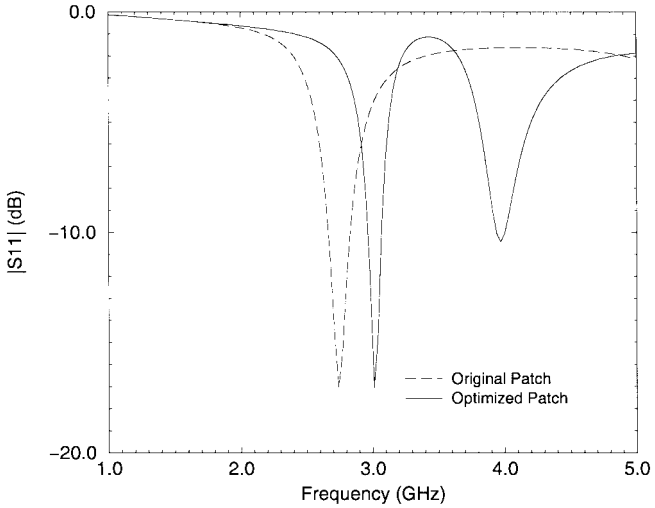

Fig. 8. Calculated $S11$ for the dual-band patch antenna before and after GA/MoM optimization.

In addition to the use of the fitness function of (9), a constraint was placed on the GA/MoM search to insure that only symmetrical structures were produced. In this case, symmetry was enforced about the y-axis. This constraint is easily implemented by controlling the mapping between the chromosome and the physical patches such that a group of patches are equated with a given bit within the GA chromosome. Grouping of patches was also used in the previous example to insure that pairs of triangles and not individual triangle were used in the optimization process.

The results of the best individual from the GA/MoM optimization in terms of magnitude $S11$ are shown in Fig. 8 along with the return loss for the original patch prior to optimization.

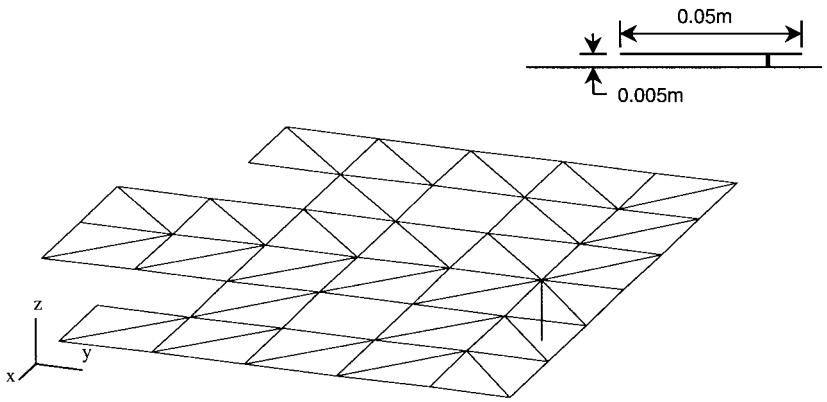

Fig. 9. Dual-band GA optimized patch antenna structure (ground plane is not shown).

As can be seen, GA/MoM again found an acceptable design given the requirement for dual-band operation. Even though a shift from the original operating frequency was required in addition to the production of a second match point, GA/MoM was able to achieve a VSWR of at least 2 : 1 at both 3.0 and 4.0 GHz. It should be noted that the resonant frequency of the original patch antenna was selected to be below that of both design goal frequencies to insure that removal of metal would have a chance of leading to a successful design.

The structure that resulted from the dual-band optimization is shown in Fig. 9. The imposed symmetry is evident in the structure unlike the broad-band case of Section IV.

Since the MoM results provide the surface current distribution on the patch antenna, it is an easy matter to calculate the radiation pattern from the MoM results. The patterns before and after optimization for the principle plane cuts are presented in Fig. 10 at 3.0 GHz. Fig. 10(a) is a plot of the $\phi = 0°$ plane cut. Fig. 10(b) is a plot of the $\phi = 90°$ plane cut. As expected by virtue of the imposed symmetry, the patterns are symmetrical with respect to the y-axis. Also the antenna exhibits good cross-polarization performance at broadside. That the pattern has improved is attributable to the improvement in the match at 3.0 GHz with respect to the original patch antenna.

The dual-band optimized patch antenna was also modeled using finite-difference time-domain (FDTD). The FDTD model had a finite ground plane and was fed with a coaxial and wire feed similar to the method that would be used in an actual antenna.

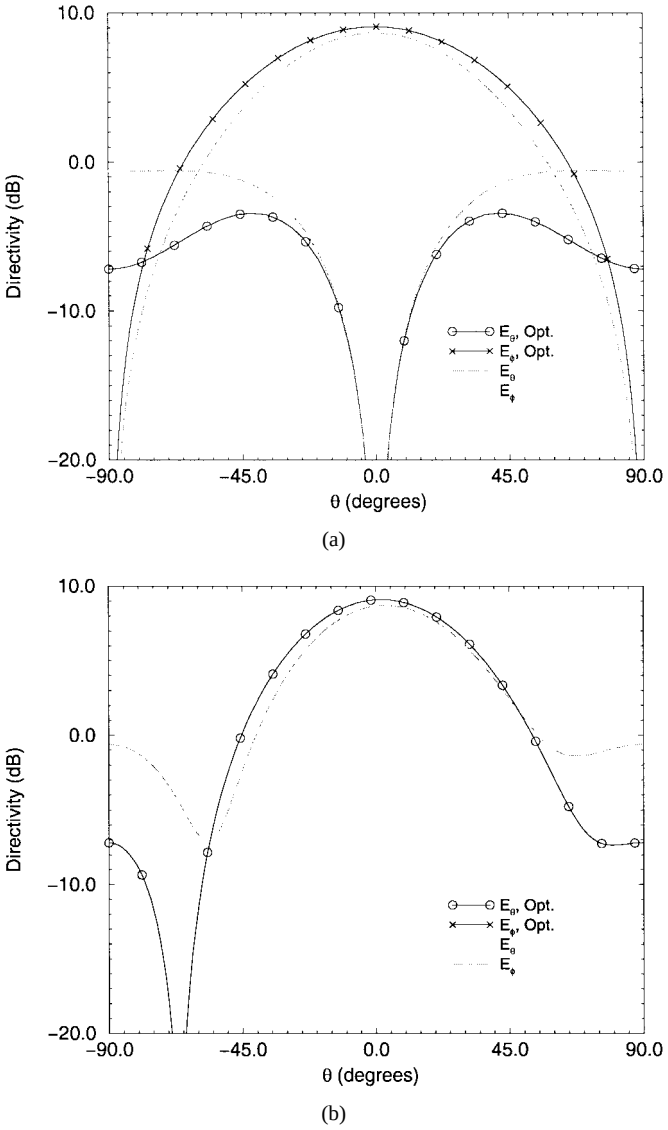

Fig. 10. Principle plane radiation patterns of the original patch antenna and the dual-band optimized patch. (a) $\phi = 0°$ plane cut. (b) $\phi = 90°$ plane at 3.0 GHz (the $E\phi$ components for $\phi = 90$ are below the plotted range).

A. Measured Results of Optimized Patch Antenna

A prototype of the dual-band optimized antenna was constructed. The prototype patch was made out of 0.304 cm copper foil cut to the dimensions determined by the GA optimization. The patch was connected to and fed by a wire feed which was connected to a 50-Ω SMA connector in the ground plane. The ground plane consisted of a copper clad fiberglass board 19.1 cm long and 15.2 cm wide. A photograph of the prototype antenna is provided in Fig. 11.

The prototype antenna was tested by mounting the antenna in the UCLA RF anechoic chamber. An HP-8510B Network Analyzer was used to measure the input return loss $S11$. The measured magnitude $S11$ data are presented in Fig. 12. Also plotted in Fig. 12 are the MoM and FDTD modeled magnitude $S11$ results.

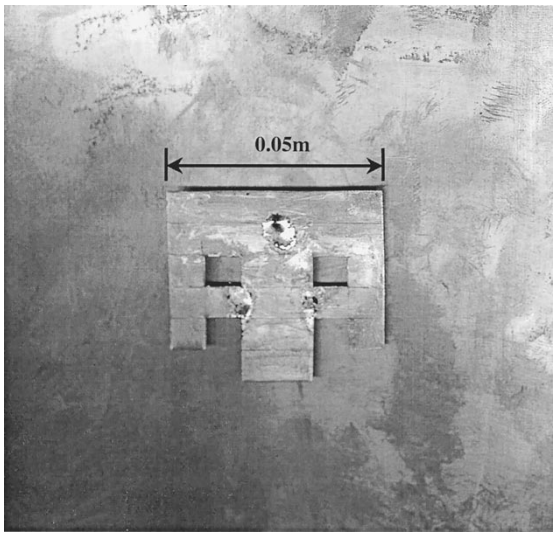

Fig. 11. Photograph of the prototype dual-band GA optimized antenna.

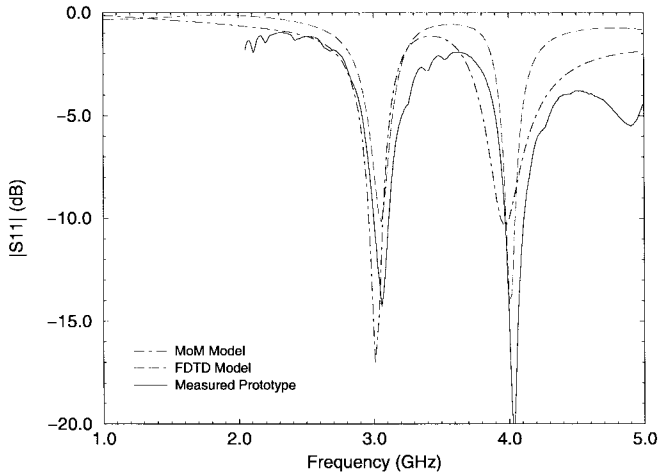

Fig. 12. Measured and modeled $|S11|$ performance for the GA optimized dual-band antenna.

The measured and MoM modeled performance agree remarkably well. The prototype antenna exhibited a slight shift in the locations of the two operational bands. In the measured results, a peak $|S11|$ of -14.3 dB at 3.06 GHz and -20.3 dB at 4.03 GHz. This represents less than a 60 MHz deviation from the goal at 3.0 GHz and less than 30 MHz at 4.0 GHz. Moreover, the width of the match regions in the MoM results and the measured results for the prototype were in close agreement.

B. Investigation of Dual-Band Patch Operation

Having developed a working dual-band patch antenna, it is interesting to consider how and why the structure produces the observed characteristics. In this section, the details of an investigation into the performance of the dual-band patch are presented. The approach followed in the investigation was to attempt to identify and quantify the effects of various substructures that make up the dual-band patch. It should be noted that the GA/MoM probably did not proceed in the manner described below. This investigation merely seeks to provide an understanding of the final result and not the route taken by GA/MoM to arrive at the result.

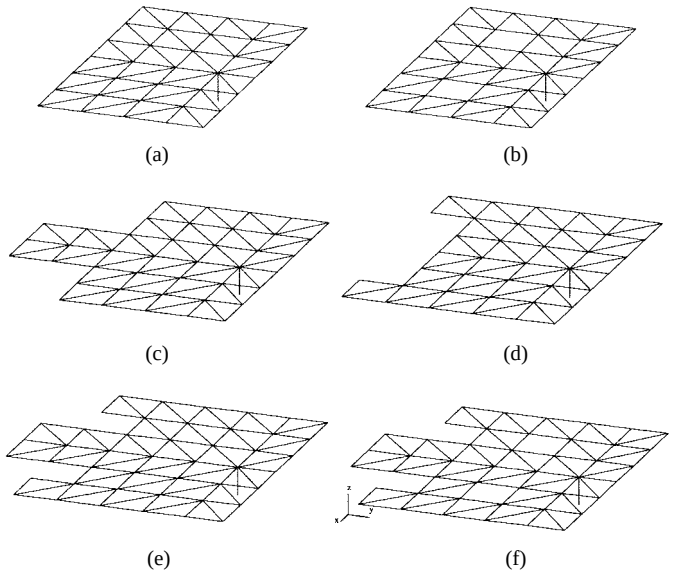

Fig. 13. Several substructures of the dual-band patch antenna are readily identifiable including: (a) the main body without holes; (b) the main body with holes; (c) the main body with the central tab; (d) the main body with the two small tabs; (e) the main body plus the large and small tabs; and (f) the complete dual-band antenna with tabs and holes.

With some thought, a series of substructures can be readily identified in the dual-band patch. These substructures include the main body of the patch, the central stub, the two smaller outside stubs, and the holes in the main body. Each of these substructures was analyzed using MoM assuming an infinite ground plane as before.

Fig. 13(a) and (b) are illustrations of the main body portion of the dual-band with and without holes showing the triangular MoM grid. Fig. 14 shows the magnitude $S11$ results for the main body of the dual-band patch. The analysis was conducted with and without the holes. As can be seen, the main body has a response that approximates the upper resonance of the GA/MoM derived antenna. The presence of the holes improves both the location and depth of the exhibited resonance. The $|S11|$ performance of the complete dual-band patch structure is provided for comparison in Fig. 14.

Next, the effect of the large and small tabs was investigated. Fig. 15 is a plot of the $|S11|$ obtained from MoM analysis of the two structures illustrated in Fig. 13(c) and (d). In the case where the small tabs are present but the holes and central tab are absent [Fig. 13(c)], the resonance of the main body of the patch is further enhanced and the resonance frequency is seen to be located at 4.0 GHz. The addition of the central tab without the smaller tabs and the holes [Fig. 13(d)] moves the resonance to near that of the 3.0-GHz design frequency.

The combined performance of the central tab, small tabs, and patch main body without holes is plotted in Fig. 16. Having the central tab and small side tabs present simultaneously produces a pair resonance as observed in the optimized dual-band. The resonance frequencies of the pair of resonances are shifted approximately 100 MHz from the desired 3.0- and 4.0-GHz design frequencies. It is only with the addition of the

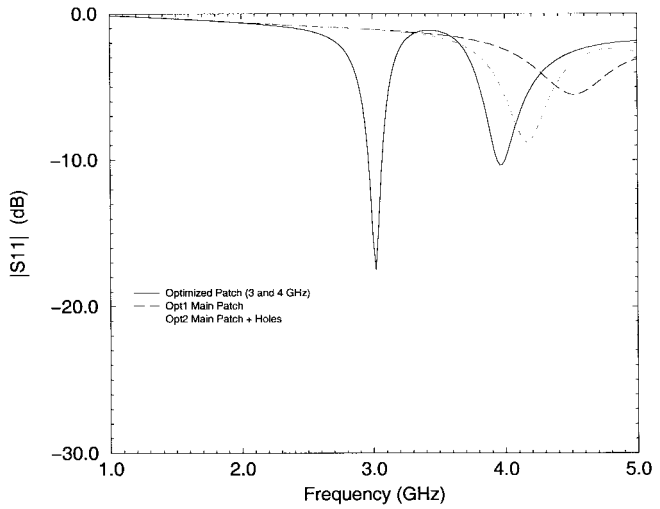

Fig. 14. Magnitude $S11$ results for the main body with and without holes compared to that of the complete dual-band patch antenna.

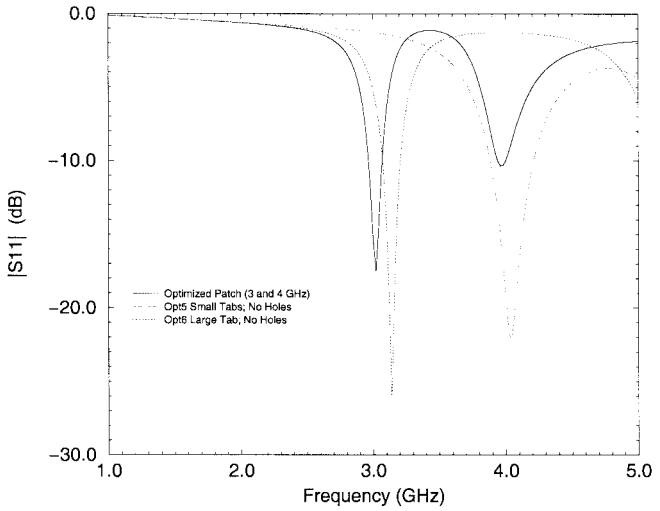

Fig. 15. Magnitude $S11$ results for the main body with the central tab and the main body with the smaller tabs both without holes as shown in Fig. 13(c) and (d).

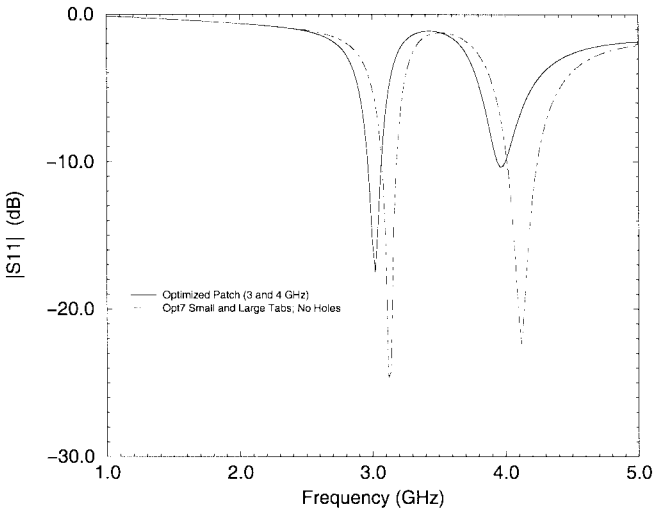

Fig. 16. Magnitude $S11$ results for the main body with both the central tab the smaller tabs without holes, as shown in Fig. 13(e), and the results of the complete dual-band patch structure, shown in Fig. 13(f).

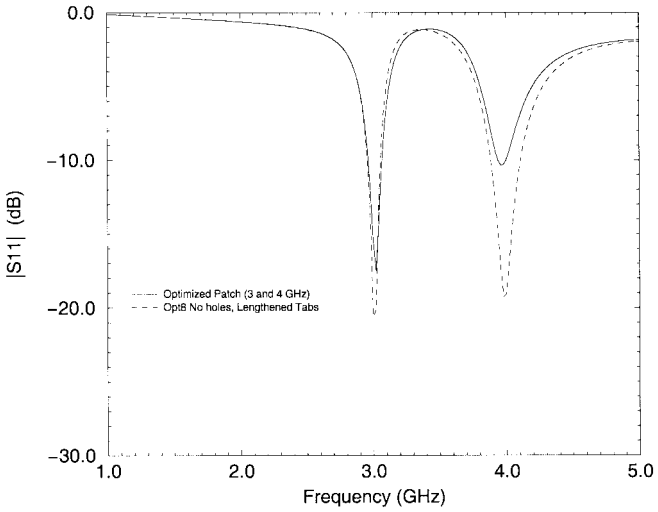

Fig. 17. The GA/MoM results can be improved by slightly lengthening the tabs and leaving out the holes.

holes that resonance at 3.0 and 4.0 GHz is finally achieved. The goal is achieved at the cost of reduced levels of return loss match, however.

The GA successfully discovered a solution that meets the design goals but the performance shown in Fig. 16 indicates that a better structure than that found by GA might, in fact, be possible. If the central tab is lengthened by 1.5 mm and the two side tabs are lengthened by 1.0 mm a better result than that obtained by GA is achieved. The $|S11|$ performance in this case is plotted in Fig. 17. The resonances are at the desired 3.0 and 4.0 GHz. The peak $|S11|$ is better than -18 dB for both bands.

Of course, GA/MoM was only allowed to add or remove patches of metal with preassigned dimensions. Changing the size of the patches was prohibited due to the *mother* matrix approach of GA/MoM. Of course smaller patches could have been used. The ability of GA to find a solution that is close to the goal makes it possible for the researcher to get close to an ultimate design by using GA/MoM. The design engineer can then apply good engineering practice to tweak the design for better performance.

VI. Conclusion

An efficient method for the integration of GA optimization with MoM for patch antenna design has been presented. A DMM method was introduced using a *mother* matrix/structure that yields significant reductions in the GA optimization time when MoM is employed in determining the fitness values. GA/MoM was applied successfully in the design of a broad-band patch antenna. The broad-band patch antenna while less than $1/2$ wavelength in extent exhibited greater than 20% bandwidth although the pattern may not be suitable for some applications. A second application of the GA/MoM optimization of a patch antenna was also presented in which a dual-band patch antenna was developed. The dual-band patch antenna design was built and the impedance charac-

teristics where measured. The prototype antenna impedance performance and the predictions from the MoM analysis agreed closely. FDTD analysis of the dual-band patch yielded impedance performance predictions that also agreed well with the measured results. An attempt to understand the operation of the dual-band antenna was also presented.

The resulting antenna structures produced by GA/MoM perform well and are nonintuitive, perhaps even surprising, designs. The principle advantage in using GA/MoM is that the process largely automates the design of new integrated antennas. In addition, the possibility of finding entirely new unanticipated antenna design is strongly evident in the nonintuitive nature of the resulting designs. This opens the possibility that the application of methods such as GA/MoM can produce rapid advances in the performance capabilities of small, cost effective, integrated antennas for wireless communication system application.

REFERENCES

[1] J. M. Johnson and Y. Rahmat-Samii, "The tab monopole," *IEEE Trans. Antennas Propagat.*, vol. 45, pp. 187–188, Jan. 1997.

[2] A. John and R. H. Jansen, "Evolutionary generation of (M)MIC component shapes using 2.5 D EM simulation and discrete genetic optimization," in *Proc. IEEE MTT-S Int. Microwave Symp.*, San Francisco, CA, June 1996, vol. 2, pp. 745–748.

[3] B. Kemp, S. J. Porter, and J. F. Dawson, "Optimization of wire antennas using genetic algorithms and simulated annealing," in *Proc. Appl. Computat. Electromagn. Symp.*, Monterey, CA, Mar. 1997, vol. II, pp. 1350–1357.

[4] E. E. Altshuler and D. S. Linden, "Wire-antenna designs using genetic algorithms," *IEEE Antennas Propagat. Mag.*, vol. 39, pp. 33–43, Apr. 1997.

[5] J. M. Johnson and Y. Rahmat-Samii, "Genetic algorithms in engineering electromagnetics," *IEEE Antennas Propagat. Mag.*, vol. 39, pp. 7–25, Aug. 1997.

[6] Y. Rahmat-Samii and E. Michielssen, Eds., *Electromagnetic Optimization by Genetic Algorithms*. New York: Wiley, 1999.

[7] R. L. Haupt, "An introduction to genetic algorithms for electromagnetics," *IEEE Antennas Propagat. Mag.*, vol. 37, pp. 7–15, Apr. 1995.

[8] J. M. Johnson and Y. Rahmat-Samii, "Genetic algorithm optimization and its application to antenna design," in *Proc. IEEE Antennas Propagat. Soc. Int. Symp.*, Seattle, WA, June 1994, pp. 326–329.

[9] B. Chambers and A. Tennant, "Design of wideband Jaumann radar absorbers with optimum oblique incidence performance," *Electron. Lett.*, vol. 30, no. 18, pp. 1530–1521, 1994.

[10] S. E. Haupt and R. L. Haupt, "Phase-only adaptive nulling with a genetic algorithm," *IEEE Aerosp. Conf. Proc.*, Aspen, CO, Feb. 1997, vol. 3, pp. 151–160.

[11] D. V. Sidorovitch, D. Maiwald, and J. F. Bohme, "Accuracy of wave parameter estimation using polarization sensitive arrays," in *Proc. EUSIPCO'94. 7th Eur. Signal Processing Conf.*, 1994, vol. 1, pp. 359–362.

[12] G. F. Uler, O. A. Mohammed, and Chang-Seop Koh, "Utilizing genetic algorithms for the optimal design of electromagnetic devices," *IEEE Trans. Magn.*, vol. 30, pt. 1, pp. 4296–4298, Nov. 1994.

[13] D. E. Goldberg and K. Deb, "A comparative analysis of selection schemes used in genetic algorithms," *Foundations of Genetic Algorithms*. San Mateo, CA: Morgan Kaufmann, 1991, pp. 69–93.

[14] D. E. Goldberg, *Genetic Algorithms in Search, Optimization and Machine Learning*. Reading, MA: Addison-Wesley, 1989.

[15] A. J. Poggio and E. K. Miller, "Integral equation solutions of three-dimensional scattering problems," in *Computer Techniques for Electromagnetics*, R. Mittra, Ed. New York: Hemisphere, 1987.

[16] S. M. Rao, D. R. Wilton, and A. W. Glisson, "Electromagnetic scattering by surfaces of arbitrary shape," *IEEE Trans. Antennas Propagat.*, vol. AP-30, pp. 409–418, May 1982.

[17] R. E. Hodges and Y. Rahmat-Samii, "An iterative current-based hybrid method for complex structures," *IEEE Trans. Antennas Propagat.*, vol. 45, pp. 265–276, Feb. 1997.

[18] P. Parhami, Y. Rahmat-Samii, and R. Mittra, "Technique for calculating the radiation and scattering characteristics of antennas mounted on a finite ground plane," in *Proc. Inst. Elect. Eng.*, vol. 124, pp. 1009–1016, Nov. 1977.

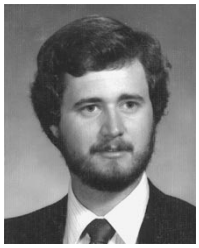

J. Michael Johnson (M'97) received the B.S. and M.S.E. degrees from the University of California, Irvine, in 1980 and 1983, respectively, and the Ph.D. degree in electrical engineering from the University of California, Los Angeles, in 1997.

He is an Assistant Professor of Electrical Engineering at the University of Nevada, Reno. He has worked for both large and small companies including Hughes Aircraft Company, Newport Beach, CA, from 1980 to 1984, where he was involved in advanced hybrid microelectronics, Lockheed Missiles and Space, Sunnyvale, CA, from 1984 to 1986, as a Satellite Receiver Designer, and for Deskin Research Group, Santa Clara, CA, from 1988 to 1989. Most recently, he was employed by Condor Systems, San Jose, CA, from 1986 to 1988 and 1989 to 1991, as a Microwave Design Engineer and Senior Staff Systems Engineer. Condor Systems is a major supplier of sophisticated electronic warfare equipment and systems and one of the fastest growing companies of its kind. During his tenure with Condor Systems, he was instrumental in the conceptualization, development, and marketing of several of the company's major product lines. In 1991 he returned to academia at UCLA, where he has specialized in computational electromagnetics with an emphasis in optimization techniques such as genetic algorithms (GA) and analysis techniques such as finite-difference time-domain (FDTD) methods. He has authored several book chapters, numerous journal, and conference articles, and holds a U.S. patent.

Dr. Johnson is a registered U.S. patent agent. He is the founder and president of North Shore Associates, Reno, NV, founded in 1994. North Shore Associates provides electrical engineering consulting and patent preparation/prosecution services for a variety of high technology clients. He was the Registration Chair and a session organizer for the 1999 and 1998 IEEE Aerospace Conferences and was Assistant Program Chair and a cosession organizer for the 1997 IEEE Aerospace Conference. In 1999 Dr. Johnson was appointed PACE Chair for the national IEEE Antennas and Propagation Society.

Yahya Rahmat-Samii (S'73–M'75–SM'79–F'85), for a photograph and biography, see p. 583 of the March 1999 issue of this TRANSACTIONS.